Tracking the interaction between injected CO2 and reservoir fluids using noble gas isotopes in an analogue of large-scale carbon capture and storage

Applied Geochemistry 78 (2017) 116–128

Contents lists available at ScienceDirect

Applied Geochemistry

journal homepage: www.elsevier.com/locate/apgeochem

Tracking the interaction between injected CO_2 and reservoir fluids using noble gas isotopes in an analogue of large-scale carbon capture and storage

Domokos Györe [a, *], Stuart M.V. Gilfillan [b], Finlay M. Stuart [a]

[a] Isotope Geosciences Unit, Scottish Universities Environmental Research Centre, East Kilbride G75 0QF, UK
[b] School of GeoSciences, University of Edinburgh, Edinburgh EH9 3JW, UK

ARTICLE INFO

Article history:
Received 7 September 2016
Received in revised form
16 December 2016
Accepted 21 December 2016
Available online 27 December 2016

Editorial handling by Prof. M. Kersten.

Keywords:
Carbon capture and storage
Geological storage
Geochemical tracing
Carbon isotope
Noble gas isotope
Mass spectrometry

ABSTRACT

Industrial scale carbon capture and storage technology relies on the secure long term storage of CO_2 in the subsurface. The engineering and safety of a geological storage site is critically dependent on how and where CO_2 will be stored over the lifetime of the site. Hence, there is a need to determine how injected CO_2 is stored and identify how injected CO_2 interacts with sub-surface fluids. Since July 2008 ~1 Mt of CO_2 has been injected into the Cranfield enhanced oil recovery (EOR) field (MS, USA), sourced from a portion of the natural CO_2 produced from the nearby Jackson Dome CO_2 reservoir. Monitoring and tracking of the amount of recycled CO_2 shows that a portion of the injected CO_2 has been retained in the reservoir. Here, we show that the noble gases (^{20}Ne, ^{36}Ar, ^{84}Kr, ^{132}Xe) that are intrinsic to the injected CO_2 can be combined with $CO_2/^3He$ and $\delta^{13}C_{CO2}$ measurements to trace both the dissolution of the CO_2 into the formation water, and the interaction of CO_2 with the residual oil. Samples collected 18 months after CO_2 injection commenced show that the CO_2 has stripped the noble gases from the formation water. The isotopic composition of He suggests that ~0.2%, some 7 kt, of the injected CO_2 has dissolved into formation water. The $CO_2/^3He$ and $\delta^{13}C_{CO2}$ values imply that dissolution is occurring at pH = 5.8, consistent with the previous determinations. $\delta^{13}C_{CO2}$ measurements and geochemical modelling rule out significant carbonate precipitation and we determine that the undissolved CO_2 after 18 months of injection (1.5 Mt) is stored by stratigraphic or residual trapping. After 45 months of CO_2 injection, the noble gas concentrations appear to be affected by CO_2-oil interaction, overprinting the signature of the formation water.

1. Introduction

Geological storage of CO_2, either in dedicated storage sites or via the utilisation of CO_2 for enhanced oil recovery (EOR), has the potential to achieve significant reduction of CO_2 emissions (IPCC, 2005). The engineering and long-term security of geological storage sites is dependent on how and where CO_2 will be stored over the lifetime of the site. Consequently, there is a need to resolve the mechanisms by which injected CO_2 is stored, quantify the efficiency and identify how injected CO_2 interacts with in-situ subsurface fluids. This demands the development of CO_2 monitoring and verification techniques (Haszeldine et al., 2005; Scott et al., 2013).

Several models of CO_2 flow and the consequent changes in physico-chemical parameters of reservoir fluids have been developed (e.g. Arts et al., 2004; Emberley et al., 2005; Knauss et al., 2005; McCraw et al., 2016; White et al., 2005). Whilst the majority of monitoring studies have relied on seismic surveys to image the free phase CO_2 plume, the technique cannot resolve the amount of CO_2 dissolved into the formation reservoir within a storage site (Scott et al., 2013). A wide range of geochemical tracing techniques have been developed to track the movement and storage of injected CO_2 (Humez et al., 2014), yet there is an outstanding need to develop a robust tool which can resolve the amount of CO_2 dissolved into the formation water within a storage site.

The isotopic composition of CO_2 ($\delta^{13}C$and $\delta^{18}O$) has been widely used to trace injected gas and track its interaction with reservoir rock and formation water as well as constrain the mechanism of storage (e.g. Assayag et al., 2009; Johnson et al., 2011, 2014; Lu et al., 2012b; Myrttinen et al., 2010; Serno et al., 2016; Raistrick et al., 2006). Both $\delta^{13}C$ and $\delta^{18}O$ measurements have also been used as

* Corresponding author.
E-mail address: Domokos.Gyore@glasgow.ac.uk (D. Györe).

http://dx.doi.org/10.1016/j.apgeochem.2016.12.012
0883-2927/

a leak detection tool (e.g. Mayer et al., 2015). However, in cases where the stable isotopic composition of injected and reservoir gas end-members is similar, the stable isotope measurements must be combined with other techniques in order to provide unique tracers of the CO_2 (Sherwood Lollar et al., 1997; Wycherley et al., 1999). Chemical tracers such as deuterated hydrocarbons (e.g. CD_4), perfluorocarbons (PFCs) and sulphur-hexafluoride (SF_6) have been added to CO_2 to determine breakthrough time and fluid interactions of injected gases in reservoirs (Boreham et al., 2011; Lu et al., 2012a; Stalker et al., 2015). However, they are prohibitively expensive to be considered for industrial scale deployment (Nimz and Hudson, 2005), technically difficult to inject, and both PFC's and SF_6 are potent greenhouse gases which will add to the greenhouse gas risk of the site should any leakage occur.

The noble gases (He, Ne, Ar, Kr and Xe) are chemically unreactive but have different solubility in fluids, so act as excellent tracers of physico-chemical processes that have affected near-surface fluids. Noble gases in natural CO_2-rich reservoirs have been used to resolve the origin and fate of CO_2 (e.g. Ballentine et al., 1991; Ballentine et al., 2001; Battani et al., 2000; Kennedy et al., 1988; Marty et al., 1991; Sherwood Lollar et al., 1994) that can be considered to be analogues for artificial long-term geologic storage (Haszeldine et al., 2005). More recent works have focused on how CO_2 has been stored in reservoirs over geological timescales (Gilfillan et al., 2008, 2009, 2011; Güleç and Hilton, 2016; Sathaye et al., 2014; Zhou et al., 2012) and in active EOR fields (Shelton et al., 2016). Inherent and artificially introduced Kr and Xe isotopes have been used to trace the movement and the time of breakthrough of injected CO_2 in carbon storage trials and CO_2-EOR fields (Freifeld et al., 2005; Giese et al., 2009; Lu et al., 2012a; Nimz and Hudson, 2005; Stalker et al., 2015) but as yet, no determination of the fate (e.g. whether the CO_2 dissolved into the formation water or was precipitated as new carbonate mineral) of injected CO_2 using these sensitive tracers has been undertaken.

Naturally occurring noble gases present in the CO_2 injected into the Cranfield EOR field (MS, USA), have recently been used to identify the loss of free phase CO_2 from the free supercritical phase (Györe et al., 2015). Here, we present new ^{84}Kr and ^{132}Xe data from gases sampled 18 and 45 months after the CO_2 injection commenced and combine them with ^{20}Ne, ^{36}Ar, $CO_2/^3He$ and $\delta^{13}C_{CO2}$ data from Györe et al. (2015) to trace and quantify the loss of CO_2 into the formation water, and its interaction with the residual oil in the reservoir. We find that measurements of ^{20}Ne, ^{36}Ar, $CO_2/^3He$ and $\delta^{13}C_{CO2}$ combined with ^{84}Kr, ^{132}Xe measurements from the Cranfield EOR field provides an excellent analogue of how similar techniques could be applied to quantify the fate of CO_2 injected into an engineered CO_2 storage site.

2. The Cranfield Enhanced Oil Recovery (EOR) field

The Cranfield oil field is located in Adams and Franklin counties of south-western Mississippi, United States. The oil reservoir is a 15–25 m thick conglomerate and sandstone of the Upper Cretaceous Lower Tuscaloosa Formation, at ~3 km below surface level. The field is a four-way closure, 6.4 km diameter dome structure. The geology and the history of primary oil recovery as well as the experiments conducted there as part of the Southeast Regional Carbon Sequestration Partnership (SECARB) are described in previous studies (e.g. Hosseini et al., 2013; Hovorka et al., 2013; Lu et al., 2012a, 2012b, 2013).

The EOR operation commenced in July 2008, and consists of the transport and injection of CO_2 from the Jackson Dome natural CO_2 reservoir (MS, USA). Prior to CO_2 injection there had only been minor water injection into the field since its abandonment in 1966. The methane, which had been co-produced with oil, was re-injected to maintain reservoir pressure during production. At end of the oil production, this methane cap was produced and then the field was abandoned. The CO_2-EOR operation consists of only CO_2 injection, with no water alternating gas (WAG) injection (Hovorka et al., 2013; Lu et al., 2012b). This is rather unusual for a CO_2-EOR field, which makes Cranfield an ideal analogue for a large-scale CO_2 storage project (Lu et al., 2012b). As injected CO_2 migrated through the field, pressure increased and CO_2 dissolved into oil and water, and the CO_2-oil mixture migrated to production wells, where CO_2, brine, oil and hydrocarbon gases were produced. Produced fluids are separated and the oil is sent to the market, produced water is injected in a different zone for disposal, and the recovered CO_2 (plus some produced hydrocarbon gases) is re-injected (Choi et al., 2013). As the amount of recycled gas has increased, additional injection and production wells were brought into operation, moving from the northwest part of the field in a clockwise direction over several years. The rate of produced gas recycling has increased with time, rising from ~10% (by mass) at the end of 2009 to ~30% by early 2012.

A CO_2 monitoring research programme has been funded primarily by the US DOE as part of the SECARB. This has included surface monitoring of CO_2 in soil gases using the process-based method (Romanak et al., 2012), fluid flow and storage capacity modelling in the reservoir, seismic surveying to image the injected CO_2 and an extensive programme of monitoring in a dedicated part of the field, known as the Detailed Area of Study (DAS) site (Fig. 1) (Alfi and Hosseini, 2016; Commer et al., 2016; Hovorka et al., 2013

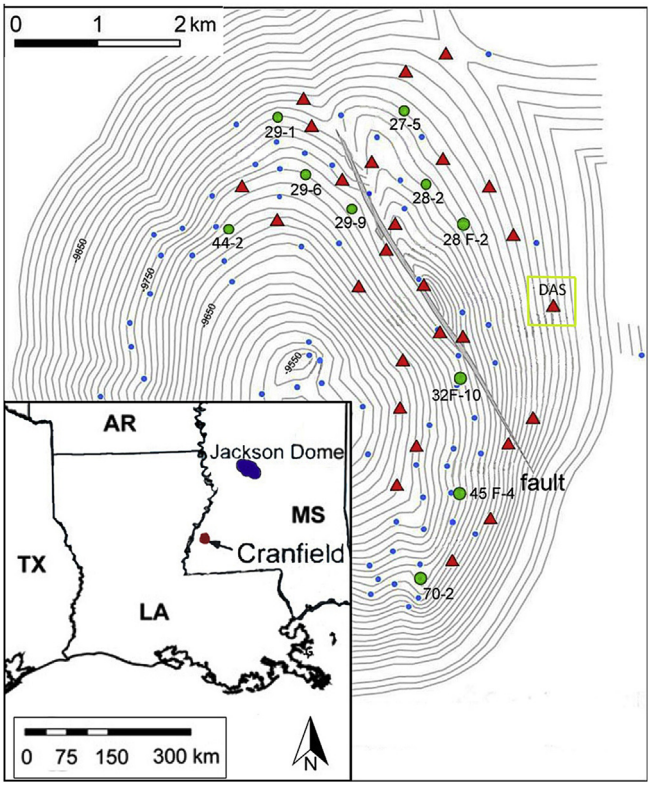

Fig. 1. The map of the Cranfield EOR field (Mississippi, USA). The grey contour shows the depth of the oil-water contact in feet (1 m = 3.28 feet). The red triangles and green circles identify the surficial location of the injection wells and production wells respectively. The production wells sampled in this study are identified by their sample ID, while other wells in the field that were not sampled are identified as blue circles. The inset figure shows the location of the Cranfield site and the Jackson Dome field, from where the CO_2 is pumped for oil recovery. DAS: Detailed Area of Study. Redrawn after Lu et al. (2012b). (For interpretation of the references to colour in this figure legend, the reader is referred to the web version of this article.)

and references therein). In December 2009 and April 2010, artificial Kr, Xe and SF_6 tracers were injected into the CO_2 stream through well 31F-1 (API: 2303721488) at the initial rate of 300 kg/min below the oil-water contact (Lu et al., 2012a). Produced CO_2 chemistry was monitored at well 31F-2 (API: 2303721485) and well 31F-3 (API: 2303721486), 65 m and 112 m east of the injection well respectively. Unfortunately, Xe arrival was not reported due to measurement issues but it was found that Kr reached wells 31F-2 and 31F-3 in ~317 and 245 h after the start of injection, with SF_6 arrival 26 h earlier in both cases (Lu et al., 2012a).

3. Sampling and analytical techniques

Gases from injection and production wells from the lower Tuscaloosa reservoir were sampled by the established copper tube method as described in Györe et al. (2015). The samples were collected in December 2009 and March 2012, 18 and 45 months after the start of CO_2 injection in early July 2008. The injected CO_2 stream was sampled during both campaigns at one injection well head (following injection of some ~3 Mt of 'new' CO_2 from Jackson Dome which was mixed with gas produced from the field prior to reinjection). Seven and eight production wells were sampled in 2009 and 2012 respectively. Five production wells, out of the seven sampled in 2009, were in operation in 2012 and were re-sampled (Fig. 1). The DAS site was sampled separately in December 2009 and April 2010. Samples were collected six times between the 4th and the 19th of December from observation well 31F-2, and three times between the 4th and the 21st of December from observation well 31F-3. The injected tracer was also sampled prior to its introduction to the DAS site.

Gases collected from the lower Tuscaloosa reservoir were purified in a purpose built all-metal ultra-high vacuum system (Györe et al., 2015). An aliquot of the pre-cleaned gas was taken for Kr and Xe analysis and was purified by exposure to four SAES GP50 ZrAl alloy getter held at 250 °C for 10 min. This was followed by equilibration to a liquid nitrogen cooled charcoal cold finger (held at −196 °C) for 10 min which retained Ar, Kr and Xe. He and Ne were then removed by pumping. The charcoal cold finger was then warmed to around −80 °C using an acetone-dry-ice slush mixture for 10 min and the gas was then administered to the mass spectrometer for analysis. The heat up step released 10–50% of the Kr and no Xe. Finally, the residual Ar was pumped and the charcoal was warmed up to ~80 °C by hot water for 10 min (Pujol et al., 2011) and the remaining Kr and Xe was analysed in the mass spectrometer. The final heat up step removed all remaining noble gases from the charcoal finger.

The concentration of ^{84}Kr and ^{132}Xe were measured using an MAP 215-50 noble gas mass spectrometer operated in static mode. Kr and Xe beam intensities were determined on a Burle channeltron electron multiplier in pulse counting mode. The reproducibility of the analysis was determined by repeated analysis of air. The absolute amount of ^{84}Kr and ^{132}Xe is based on a peak height comparison with the calibration bottle, using the composition of air (Berglund and Wieser, 2011; Ozima and Podosek, 2001). Blanks were negligible for all isotopes. The isotopic composition of the Kr and Xe tracers injected into the DAS site and the $^{84}Kr/^{36}Ar$ and $^{132}Xe/^{36}Ar$ of the DAS observation wells were analysed on a VG 5400 noble gas mass spectrometer at the University of Rochester by the method described by Poreda and Farley (1992).

4. Results

4.1. DAS observation wells

The noble gas tracers injected into the DAS site in both December 2009 and April 2010 originated from a single 300 L cylinder, which contained 40% Kr, 10% Xe and 50% N_2. The isotopic composition of the Kr and Xe from both injection events is almost identical to air (Table 1). The injected gas had $^{84}Kr/^{132}Xe$ of 8.49 ± 0.05 and 7.18 ± 0.04 in 2009 and 2010 respectively. $^{84}Kr/^{36}Ar$ and $^{132}Xe/^{36}Ar$ ratios of the DAS gas are summarised in Table 2. The lowest $^{84}Kr/^{36}Ar$ (0.0029) and $^{132}Xe/^{36}Ar$ (0.0036) were observed in the first sample from well 31F-2 on 4th December 2009 prior to CO_2 breakthrough. The highest $^{84}Kr/^{36}Ar$ (0.85) and $^{132}Xe/^{36}Ar$ (0.25) was measured in gas from well 31F-2 sampled on the 17th of December 2009 indicating maximum breakthrough of the injected tracers.

4.2. Production wells

The $^{4}He/^{20}Ne$ of all samples is several orders of magnitude higher than the atmospheric value and therefore atmospheric air contamination during sampling or analysis can be ruled out (Györe et al., 2015). The composition of the Jackson Dome CO_2 which was sampled directly from the pipeline cannot be used due to a CO_2 hydrate build up causing noble gas fractionation during sampling (Györe et al., 2015). The composition of the Jackson Dome CO_2 end members of $^{20}Ne/^{36}Ar$ and $^{84}Kr/^{36}Ar$ was obtained using average values of gas sampled from the CO_2 field (Zhou et al., 2012) after the method outlined by Györe et al. (2015) (Table 3). Zhou et al. (2012) did not measure Xe isotopes. However, the $^{132}Xe/^{36}Ar$ (0.0014) can be determined from the intersection of the best linear fit according to the least square method along all of the $^{84}Kr/^{36}Ar$ and $^{132}Xe/^{36}Ar$ data from the Cranfield lower Tuscaloosa reservoir and the $^{84}Kr/^{36}Ar$ value of the Jackson Dome gas (Fig. 2).

The $^{84}Kr/^{132}Xe$ measured in production wells from the lower Tuscaloosa reservoir in 2009 and 2012 is much lower than the atmospheric value of 27.8. The concentration of ^{84}Kr in injection wells decreases from $4.36 \pm 0.18 \times 10^{-10}$ to $4.05 \pm 0.17 \times 10^{-10}$, whereas the ^{132}Xe increases from $3.74 \pm 0.20 \times 10^{-11}$ to $4.38 \pm 0.23 \times 10^{-11}$ cm^3 STP/cm^3 from 2009 to 2012. In the production wells from 2009 the lowest ^{84}Kr ($3.04 \pm 0.13 \times 10^{-10}$ cm^3 STP/cm^3) and ^{132}Xe concentrations ($2.69 \pm 0.14 \times 10^{-11}$ cm^3 STP/cm^3) are from well 29-9 and the highest ^{84}Kr ($2.58 \pm 0.10 \times 10^{-9}$ cm^3 STP/cm^3) and ^{132}Xe ($1.92 \pm 0.10 \times 10^{-10}$$cm^3$ STP/cm^3) concentrations are from 28F to 2. Among production well samples from 2012, both the highest Kr ($1.38 \pm 0.06 \times 10^{-9}$ cm^3 STP/cm^3) and Xe concentrations ($1.33 \pm 0.07 \times 10^{-10}$ cm^3 STP/cm^3) are in well 28-2 and the lowest Kr ($3.41 \pm 0.14 \times 10^{-10}$ cm^3 STP/cm^3) and Xe concentrations ($3.10 \pm 0.16 \times 10^{-11}$ cm^3 STP/cm^3) are in 29-6 (Table 3).

Normalising ^{84}Kr and ^{132}Xe concentrations to ^{36}Ar allows the data to be compared to air and air saturated water (ASW) values. ASW is the calculated isotope ratio of atmosphere derived noble gases dissolved in the formation water and is calculated assuming equilibration of atmospheric air with zero salinity groundwater at the local average temperature of 16 °C and site altitude of 50 m, assuming a typical 10% excess air Ne component (Aeschbach-Hertig et al., 1999; Kipfer et al., 2002).

All $^{84}Kr/^{36}Ar$ data are above the air value (0.021). The calculated local ASW $^{84}Kr/^{36}Ar$ is 0.039. The measured $^{84}Kr/^{36}Ar$ of the Jackson Dome CO_2 is 0.021 ± 0.003. The $^{84}Kr/^{36}Ar$ of the injection stream increases with time, from 0.030 ± 0.002 to 0.044 ± 0.002 from 2009 to 2012. Among production well samples, well 29-9 2009 has the lowest value (0.030 ± 0.001) and 70-2 2012 has the highest (0.056 ± 0.003).

All $^{132}Xe/^{36}Ar$ data are also higher than the air value (0.00075). The calculated local ASW is $^{132}Xe/^{36}Ar$ is 0.0025. The $^{132}Xe/^{36}Ar$ in the injection well head gas samples increase from 0.0025 ± 0.0002 to 0.0048 ± 0.0003 between 2009 and 2012. Production well gases

Table 1
The isotopic composition of the injected Kr and Xe into the DAS site in 2009 and in 2010. The injected gas composition is almost identical to that of atmospheric air. 1σ uncertainties are in parenthesis as last significant figures. The composition of atmospheric air is after Berglund and Wieser (2011).

Ratio	Atmospheric air	Injected gas (Dec. 2009)	Injected gas (April 2010)
$^{124}Xe/^{132}Xe$ (x 10^{-3})	3.538 (11)	3.102 (30)	3.229 (1)
$^{126}Xe/^{132}Xe$ (x 10^{-3})	3.307 (7)	2.783 (45)	2.398 (1)
$^{128}Xe/^{132}Xe$ (x 10^{-2})	7.099 (3)	7.077 (19)	7.067 (1)
$^{129}Xe/^{132}Xe$ (x 10^{-1})	9.811 (3)	9.866 (18)	9.811 (9)
$^{130}Xe/^{132}Xe$ (x 10^{-1})	1.513 (1)	1.509 (9)	1.508 (2)
$^{131}Xe/^{132}Xe$ (x 10^{-1})	7.891 (1)	7.894 (9)	7.881 (8)
$^{134}Xe/^{132}Xe$ (x 10^{-1})	3.878 (1)	3.867 (10)	3.878 (6)
$^{136}Xe/^{132}Xe$ (x 10^{-1})	3.292 (2)	3.275 (22)	3.296 (4)
$^{80}Kr/^{84}Kr$ (x 10^{-2})	4.011 (18)	4.058 (64)	4.043 (1)
$^{82}Kr/^{84}Kr$ (x 10^{-1})	2.034 (5)	2.044 (26)	2.040 (1)
$^{83}Kr/^{84}Kr$ (x 10^{-1})	2.018 (3)	2.018 (17)	2.017 (2)
$^{86}Kr/^{84}Kr$ (x 10^{-1})	3.032 (7)	3.014 (40)	3.024 (3)
$^{84}Kr/^{132}Xe$ (x 10^{1})	2.775 (28)	0.849 (48)	0.718 (40)

Table 2
The isotopic composition of the DAS site gas from observation wells after the injection of the artificial tracer in December 2009. Times are given in UTC-7. 1σ uncertainties are in parenthesis as last significant figures. For well API numbers see text.

Well	Date of sampling	$^{84}Kr/^{36}Ar$ (x 10^{-1})	$^{132}Xe/^{36}Ar$ (x 10^{-2})
31F-2	4th Dec, 9:39	0.028 (2)	0.363 (20)
31F-2	4th Dec, 15:05	0.754 (37)	0.427 (23)
31F-2	12th Dec, 15:00	1.776 (56) (18)	5.288 (270)
31F-2	13th Dec, 19:00	0.853 (46)	2.903 (160)
31F-2	17th Dec, 18:45	8.499 (212)	25.547 (920)
31F-2	19th Dec, 17:00	0.573 (29)	1.872 (96)
31F-3	4th Dec, 17:38	0.754 (39)	0.503 (25)
31F-3	19th Dec, 17:30	0.285 (14)	0.781 (44)
31F-3	21st Dec, 17:00	2.666 (135)	11.613 (534)

vary between 0.0024 ± 0.0002 (Well 44-2 2009) and 0.0053 ± 0.0003 (Well 28-2 2012).

The calculated local ASW $^{20}Ne/^{36}Ar$ is 0.163. All wells, except for 28F-2 (2009) (0.148 ± 0.04), have higher $^{20}Ne/^{36}Ar$ than ASW (Györe et al., 2015), though generally lower than the air value (0.526). The $^{20}Ne/^{36}Ar$ of the Jackson Dome CO_2 is 1.129 ± 0.012 (Zhou et al., 2012). $^{20}Ne/^{36}Ar$ ratio of the injected gas decreases from 0.618 ± 0.035 to 0.547 ± 0.031 from 2009 to 2012, as a result of a greater amount of recycling of the produced gas into the injection stream. The $^{20}Ne/^{36}Ar$ of the production wells range from 0.148 ± 0.040 (28F-2 2009) to 0.637 ± 0.036 (well 29-6 from both sampling campaigns) (Györe et al., 2015).

5. Discussion

5.1. Migration of injected Kr and Xe tracers from DAS site into the Lower Tuscaloosa reservoir

The concentration of artificial ^{84}Kr in the DAS site fluids must have been ~1219 times higher than that in the lower Tuscaloosa pool (Appendix 1), and thus a small contribution of this CO_2 would significantly affect the $^{84}Kr/^{36}Ar$ of the production gases and rule out their use as natural tracers. Hence, the possibility of migration of the artificially introduced Kr and Xe from the DAS site to the main Cranfield EOR reservoir must be assessed before undertaking interpretation of the data obtained from the well head gases produced from the Tuscaloosa reservoir.

Table 3
The non-radiogenic noble gas isotopic composition of well gases from Cranfield.

Well ID	Year of sampling	Well Type	^{84}Kr (x 10^{-10})	^{132}Xe (x 10^{-11})	$^{20}Ne/^{36}Ar$	$^{84}Kr/^{36}Ar$(x 10^{-2})	$^{132}Xe/^{36}Ar$(x 10^{-3})
31F-1	2009	Injector	4.356 (181)	3.743 (196)	0.618 (35)	2.966 (167)	2.549 (165)
32F-4	2012	Injector	4.045 (168)	4.384 (230)	0.547 (31)	4.425 (249)	4.795 (310)
28–2	2009	Producer	7.278 (303)	6.835 (358)	0.345 (20)	3.862 (219)	3.627 (236)
28–2	2012	Producer	13.81 (57)	13.34 (69)	0.255 (14)	5.446 (305)	5.261 (339)
28F-2	2009	Producer	25.82 (99)	19.19 (99)	0.148 (40)	3.618 (203)	2.689 (174)
28F-2	2012	Producer	7.026 (292)	6.989 (366)	0.428 (24)	4.175 (233)	4.153 (267)
29–6	2009	Producer	3.439 (143)	3.103 (163)	0.607 (35)	2.922 (165)	2.636 (171)
29–6	2012	Producer	3.411 (142)	3.101 (162)	0.637 (36)	4.233 (238)	3.848 (249)
29–9	2009	Producer	3.041 (126)	2.691 (141)	0.637 (36)	2.860 (160)	2.531 (163)
29–1	2009	Producer	7.273 (303)	8.000 (419)	0.384 (22)	3.666 (206)	4.033 (261)
29–1	2012	Producer	6.056 (252)	5.952 (312)	0.422 (24)	3.803 (212)	3.738 (240)
27–5	2009	Producer	12.77 (53)	13.83 (72)	0.170 (15)	4.129 (280)	4.473 (289)
27–5	2012	Producer	6.723 (279)	6.865 (359)	0.448 (25)	4.792 (269)	4.893 (315)
44–2	2009	Producer	24.06 (98)	17.03 (89)	0.201 (20)	3.368 (189)	2.383 (154)
45F-4	2012	Producer	7.929 (329)	7.502 (393)	0.386 (22)	5.108 (291)	4.833 (315)
32F-10	2012	Producer	7.897 (328)	7.567 (396)	0.443 (25)	5.411 (303)	5.185 (334)
70–2	2012	Producer	8.141 (338)	7.551 (395)	0.443 (26)	5.601 (321)	5.195 (341)
Jackson Dome	NA	NA	1.782 (293)	1.800 (324)	1.129 (12)	2.126 (330)	1.400 (255)
AIR	NA	NA	6498 (5)	2340 (3)	0.526 (3)	2.077 (18)	0.748 (9)
ASW	NA	NA	NA	NA	0.163	3.897	2.480

1σ uncertainties are in parentheses as last significant figures.
Noble gas concentrations are in cm^3 STP/cm^3. Standard conditions are after Ozima and Podosek (2001) (0.101 MPa, 0 °C).
Jackson Dome values are after Zhou et al. (2012). ^{20}Ne and ^{36}Ar values of Cranfield well gases are after Györe et al. (2015).
The composition of air is after Ozima and Podosek (2001).
The geographical locations and API numbers of production wells are in Table 5.

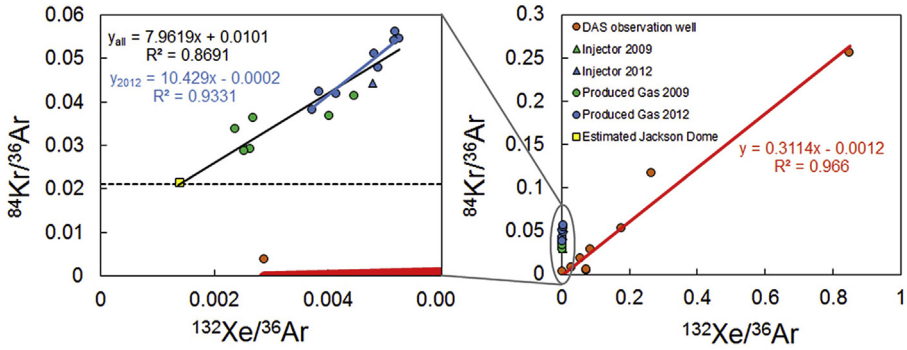

Fig. 2. The $^{84}Kr/^{36}Ar$ and $^{132}Xe/^{36}Ar$ from gases from the Cranfield field. The increase in the ratios of the DAS observation well data (right) corresponds to the presence of more Kr-Xe tracer in the sample (see Table 2). The red line shows the trend of changes in the isotopic composition due to the artificial Kr-Xe tracer injection. The production well data from 2012 (blue) from the Cranfield lower Tuscaloosa reservoir (left) show linear correlation but the trend is significantly different than that of DAS site. This confirms that the artificial tracer injection event has no influence on other parts of the reservoir. Dashed line shows $^{84}Kr/^{36}Ar$ of the Jackson Dome gas. The full dataset from the production wells can be used to estimate the $^{132}Xe/^{36}Ar$ of the Jackson Dome gas and was found to be 0.0014. Uncertainties are 1σ. (For interpretation of the references to colour in this figure legend, the reader is referred to the web version of this article.)

All production wells samples were taken from the lower Tuscaloosa reservoir between the 1st and the 4th of December 2009, with the first DAS tracer injection event taking place on 3rd December 2009. Consequently, the injected Kr and Xe into the DAS site did not have enough time to travel to the lower Tuscaloosa reservoir (Lu et al., 2012a) and cannot have affected the production wells sampled in 2009. This is also indicated by the measured $^{84}Kr/^{132}Xe$ ratios in the production wells (9.09 ± 0.78 to 13.45 ± 1.15), which are significantly higher than the DAS injected tracer (8.5) in December 2009.

The 2012 sampling campaign occurred 816 and 817 days after the first DAS injection event. The 2009 and 2012 data of $^{84}Kr/^{36}Ar$ and $^{132}Xe/^{36}Ar$ from the lower Tuscaloosa pool shows an entirely different trend than that from the DAS site (Fig. 2). This relationship provides conclusive evidence that the gases sampled in both 2009 and 2012 from the lower Tuscaloosa pool do not contain the artificial Kr and Xe tracer injected into the DAS site.

5.2. Resolving CO_2–water–oil interaction

5.2.1. Role of air-saturated water-derived noble gases in the reservoir gas

In a crustal fluid system, atmosphere-derived noble gases originate from either aquifer recharge or equilibration of formation water at the time of sediment deposition (e.g. Kipfer et al., 2002). The dissolution of CO_2 into groundwater results in the (partial) degassing of the dissolved noble gases into a free gas phase (Gilfillan et al., 2008, 2009; Zhou et al., 2012). Completed degassing of noble gases will impart an ASW-like noble gas element composition to the gas phase. Given that CO_2 injection in Cranfield causes the same degassing process, it is likely that ASW $^{20}Ne/^{36}Ar$, $^{84}Kr/^{36}Ar$ and $^{132}Xe/^{36}Ar$ will be evident in samples where there is an intense CO_2 - water interaction.

A binary mixing relationship between the injected and the reservoir gas is apparent between the $^{3}He/^{4}He$, $^{40}Ar^{*}/^{4}He$ and $^{20}Ne/^{22}Ne$ of well gases from the Cranfield EOR reservoir (Györe et al., 2015). $^{20}Ne/^{36}Ar$ ratios generally follow a similar binary mixing curve, which starts at the ASW ratio of 0.163 (Fig. 3A) indicating that the ASW is the most probable source of the atmospheric noble gases in the pre-injection reservoir. However, several samples plot below the mixing line.

The binary mixing with ASW-derived gas is much less apparent in the case of $^{84}Kr/^{36}Ar$ (Fig. 3B) and $^{132}Xe/^{36}Ar$ (Fig. 3C). The $^{84}Kr/^{36}Ar$ of the 2009 production well gases are close to the predicted mixing curve which, again, supports ASW as the source of the Kr (and ^{36}Ar) in the 2009 samples. However, all the 2012 $^{84}Kr/^{36}Ar$ plot above the theoretical mixing line. All the $^{132}Xe/^{36}Ar$ of the production well gases sampled in 2009 and 2012 (except 2009 sample of well 44-2) plot above the mixing line. These observations require the presence of a third source of noble gases (e.g. oil) and/or some process such as dissolution has fractionated the noble gases.

5.2.2. Noble gas composition of the pre-injection Cranfield reservoir gas

In order to identify the process responsible for the Kr and Xe data set, the noble gas compositions of the pre-injection reservoir fluids need to be determined. The formation water with ASW noble gas composition has been in contact with the reservoir gas (mostly CH_4) and oil without perturbation since field abandonment in 1966 and can be assumed to have reached equilibrium. If the reservoir gas and oil have not been in contact with the atmosphere since they were generated, they will not have originally contained atmospheric derived noble gases (e.g. Ballentine et al., 1996). However, on migration the hydrocarbons will have interacted with formation water.

Noble gases partition between phases according to Henry's law. Henry's constants under reservoir conditions (32.4 MPa, 120 °C, 2.5 M salinity; Lu et al. (2012b)) for Ne, Ar, Kr and Xe are calculated to be 3717, 2616, 2274 and 1967 atm kg/mol in water (Crovetto et al., 1982; Smith and Kennedy, 1983) and 337, 141, 51 and 30 atm kg/mol in light oil (Ballentine et al., 1996; Kharaka and Specht, 1988). The currently available constants for noble gas solubility in oil are for light oil with an API of 34° and heavy oil with an API of 25°. The Cranfield oil has an API of 39° (Hosseini et al., 2013). Hence, using the solubility values in light oil, we can model how the $^{20}Ne/^{36}Ar$, $^{84}Kr/^{36}Ar$ and $^{132}Xe/^{36}Ar$ ratios in formation water evolve following contact with oil and gas, assuming a closed system. Under these conditions, batch fractionation describes the fractionation of noble gases (Bosch and Mazor, 1988) using Eqs. (A.1-3) (see Appendix 2).

In order to determine the gas/water (G/W) and oil/water (O/W) ratios prior to CO_2 injection, we use the production values from well 28F-2 and 44-2, which had only been producing for a few days at the time of sampling in December 2009 (Mississippi Oil and Gas Board, MSOGB, 2015) and are considered to be representative of the reservoir prior to CO_2 injection (Györe et al., 2015). Well 28F-2 and 44-2 produced 75 and 59 m^3 water/day and 4930 and 3510 m^3 STP gas/day, respectively at the time of sampling. Neither well was an

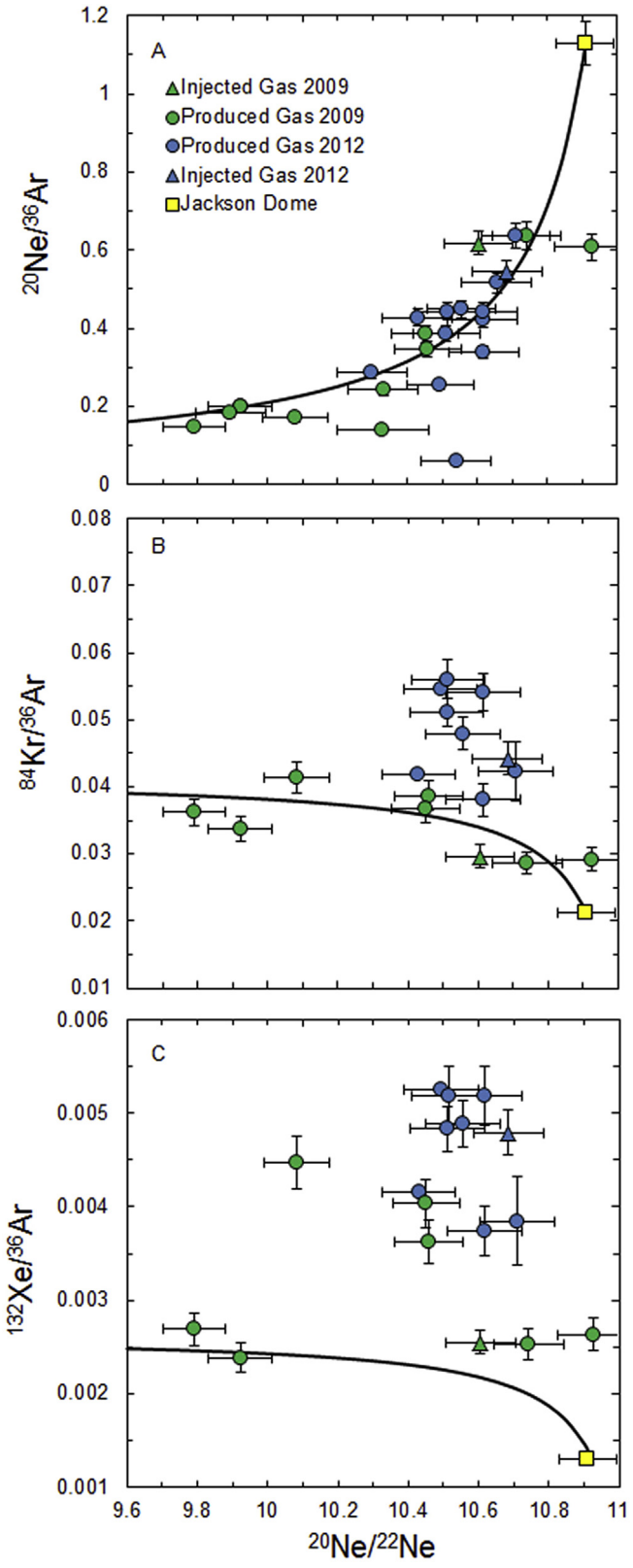

Fig. 3. The non-radiogenic noble gas ratios plotted against $^{20}Ne/^{22}Ne$ for well gases from Cranfield. Mixing curves are drawn between Jackson Dome (Zhou et al., 2012) and air-saturated water (ASW) compositions. $^{20}Ne/^{22}Ne$ and $^{20}Ne/^{36}Ar$ values are after Györe et al. (2015). $^{20}Ne/^{36}Ar$ (A) mostly follows the mixing curve. Kr (B) and Xe (C) data do not sit on the curve indicating either the presence of a third end-member or a more complicated process than mixing that causes severe fractionation. Uncertainties are 1σ.

oil producer at this time, which defines production rate of less than 0.5 m^3/day (values were recorded at the wellhead during sampling). The two wells are located on the east and the west sides of the field respectively.

Using these values, the gas (CH_4 only)/water (G/W) and oil/water (O/W) ratios prior to CO_2 injection into the field under reservoir conditions can be estimated to be 0.2 and up to 0.0075 respectively (see e.g. Ballentine et al., 1996). The pre-injection $^{20}Ne/^{36}Ar$, $^{84}Kr/^{36}Ar$ and $^{132}Xe/^{36}Ar$ in the CH_4 gas phase were calculated to be 0.181, 0.0285 and 0.0016 and in the oil phase to be 0.076, 0.0793 and 0.0075 respectively. The remaining water phase will have the composition of 0.126, 0.0327 and 0.0021 respectively (Table 4 & Fig. 4A–B).

5.2.3. Evolution of gas composition during CO_2 injection

The modelled evolution of the $^{84}Kr/^{36}Ar$ and $^{20}Ne/^{36}Ar$ gas composition by continuous CO_2 injection in the reservoir is illustrated in Fig. 4A–B. At the beginning of the injection the Jackson Dome CO_2 (Zhou et al., 2012) mixes with the pre-injection reservoir gas following the trajectory defined by line 1. The injection of CO_2 can be expected to result in degassing of noble gases from the formation water and also the oil phase. This process has been observed in a number of natural CO_2 reservoirs (Gilfillan et al., 2008; Zhou et al., 2012) and can be modelled using the batch fractionation equation. However, in Cranfield, equilibrium is unlikely to be established due to the large quantity of CO_2 injected over a relatively short period of time. Consequently, we use a mixing line that defines the evolution of noble gases between the pre-injection reservoir natural gas composition and the fully degassed water (line 2), and fully degassed oil (line 3). Complete degassing of noble gases from the formation water and the oil phase (where G/W and G/O = infinite) means the gas phase will inherit a mix of ASW and oil-derived noble gases. In this case, mixing will continue between the Jackson Dome gas and the ASW (line 4) and/or fully degassed oil composition (line 5).

The $^{84}Kr/^{36}Ar$ of the well gas samples are plotted against $^{20}Ne/^{36}Ar$ in Fig. 4A. The 2009 production well data plot within or around the triangle defined by Jackson Dome, pre-injection reservoir gas and ASW (line 1, 2 & 4). Data can be categorised into 3 groups: Well 28F-2 and 44-2 lie on the gas evolution line (line 2). This requires active and ongoing contact between the injected gas and the formation water. These are the two samples where CO_2 dissolution has been identified by Györe et al. (2015) for which the heavy noble gases were measured in this study. In both cases gas production started only a few days prior to sampling (MSOGB, 2015). Gases from wells 28-2, 29-1 and 27-5 plot on or slightly above the ASW–Jackson Dome CO_2 mixing line (line 4). These samples appear to have acquired their Ne, Ar and Kr by complete degassing of ASW and mixing between ASW and the injected Jackson Dome CO_2. Gas from the injection well 31-F1, and production wells 29-6 and 29-9 are located much closer to the Jackson Dome composition but still below the ASW–Jackson Dome mixing line (line 4). The location of these samples on the mixing line means that the amount of injected CO_2 is much higher than in the case of well 44-2 and 28F-2. Well gases 29-6 and 29-9 have the highest CO_2 concentrations of all the production wells sampled, and the noble

Table 4
Summary of the isotopic composition of the non-radiogenic noble gases in pre-injection Cranfield.

Ratio	Gas	Water	Oil
$^{20}Ne/^{36}Ar$	0.181	0.126	0.076
$^{84}Kr/^{36}Ar$ (x 10^{-2})	2.845	3.272	7.926
$^{132}Xe/^{36}Ar$ (x 10^{-3})	1.584	2.107	7.546

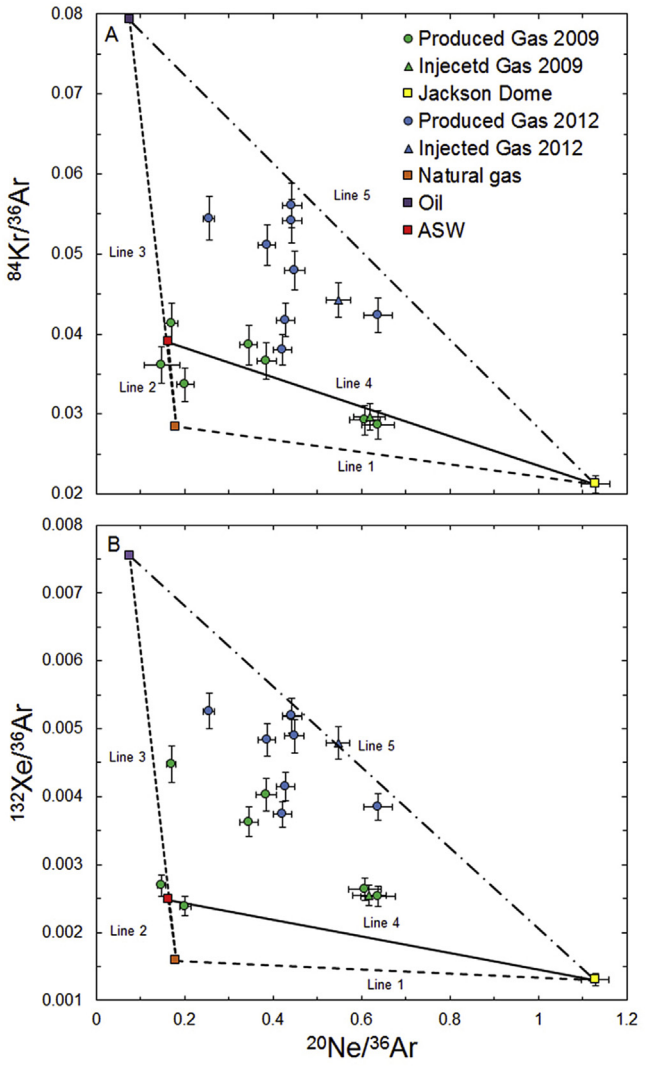

Fig. 4. The plot of $^{84}Kr/^{36}Ar$ and $^{132}Xe/^{36}Ar$ against $^{20}Ne/^{36}Ar$ for well gases from Cranfield. At the beginning of the injection, Jackson Dome gas mixes with the in-place gas along Line 1. CO_2 injection firstly degasses the water (Line 2), at the end of which mixing is described between Jackson Dome and ASW (Line 4). The likelihood of oil degassing at the early stage of CO_2-EOR operation is low due to the very low O/W ratio in the reservoir (see text), however, it cannot be completely ruled out. Later, the oil is degassed (Line 3), and in case of full degassing defines the mixing between Jackson Dome and fully degassed oil (Line 5). $^{84}Kr/^{36}Ar$ (A) values from 2009 are explained by different degree of noble gas stripping from formation water. Groups of samples show different stage of degassing. Samples on Line 2 show intense and ongoing CO_2–water contact. Samples on Line 4 show full degassing. Any data plotting within the small triangle below line 4 is due to partial degassing of ASW. $^{84}Kr/^{36}Ar$ (A) data from 2012 can be explained by partial gas stripping from oil. One sample overlaps with the fully degassed oil line (Line 5), which is the latest well that has been exposed to CO_2 flooding. Oil degassing in 2009 is unlikely due to the low O/W ratio (0.0075). All $^{132}Xe/^{36}Ar$ (B) data are within the large triangle above line 4, except for the 2012 injected gas sample. Xe data from 2009 can be explained by the high solubility of Xe in supercritical CO_2 and/or by the presence of excess Xe (see text), while the 2012 data is consistent with varying degrees of oil degassing. $^{20}Ne/^{36}Ar$ data are after Györe et al. (2015). ASW: Air Saturated Water. Uncertainties are 1σ.

gas data are also distinct, exhibiting the highest $^{3}He/^{4}He$, $^{20}Ne/^{22}Ne$, $^{40}Ar/^{36}Ar$ and $^{40}Ar^{*}/^{4}He$ ratios (Györe et al., 2015). This is consistent with the injected CO_2 flowing through the reservoir with little contact with the formation water (and oil), and supports the hypothesis that the in-place natural gas has Ne, Ar and Kr in relative proportion that is consistent with partially degassed water.

All 2012 samples plot well above the ASW–Jackson Dome mixing line (line 4) in Fig. 4A. This is explained by the presence of highly fractionated noble gases derived from the degassing of oil as a result of the continuous CO_2 injection. Only one sample (well 70-2) overlaps with the fully degassed oil mixing line (line 5). This may be explained by the time elapsed since the start of EOR operation and when those wells started oil production. This sample is from the southeast part of the field which was the last section to be subjected to CO_2 injection and was only exposed to CO_2 flooding shortly prior to sample collection in March 2012 (MSOGB, 2015). This indicates that the oil degassing by continuous CO_2 injection had reached near completion around that part of the reservoir by the time this well started producing, implying that oil degassing is a regional event across the Cranfield reservoir. All other samples show partial oil degassing as with the gas–water system. The smallest fractionation of $^{84}Kr/^{36}Ar$ is exhibited in gases produced by well 29-1, implying the least oil-CO_2 interaction.

The $^{132}Xe/^{36}Ar$ of Cranfield well gas samples is plotted against $^{20}Ne/^{36}Ar$ in Fig. 4B. The majority of the 2009 well gases plot above the line described by fully degassed water (line 4). They plot within the area that requires interaction with partially degassed oil. The three distinct groups that are identified based on the Kr/Ar data (Fig. 4A) are distinct in Ne-Ar-Xe space. The two well gases that overlap the reservoir gas evolution line (28F-2 and 44-2) in Fig. 4A are the closest to the ASW composition. The three that require fully degassed water (28-2, 29-1 and 27-5) plot together. The injection well and the production wells 29-6 and 29-9 that did not show significant interaction with the groundwater also have similar Xe/Ar ratios. The $^{132}Xe/^{36}Ar$ data of the 2012 well gases (Fig. 4B) are within the Jackson Dome–ASW and fully degassed oil triangle (Line 3, 4 & 5), which is consistent with partially degassed oil, similar to the trends observed in the $^{84}Kr/^{36}Ar$ of the 2012 gases.

There are two possible explanations for the observed Xe data. Henry's constant of Xe in supercritical CO_2–water system differs significantly from that of $CO_{2(gas)}$–water system, indicating that the solubility of Xe in supercritical CO_2 is significant (Warr et al., 2015). The Henry's constants for the other noble gases than Xe are less different. Although the experiments of Warr et al. (2015) were not completed at the pressure and temperature conditions representative of the Cranfield reservoir and they did not investigate a three component (supercritical CO_2–water–oil) system, it is likely that Xe can be extracted more efficiently than other noble gases from oil by contact with supercritical CO_2.

An alternative explanation is the presence of 'excess' Xe trapped in, or adsorbed on, organic-rich material (e.g. Kennedy et al., 2002; Torgersen and Kennedy, 1999; Torgersen et al., 2004; Zhou et al., 2005). If excess Xe is present in the Cranfield oil phase, it would either have made the oil oversaturated with respect to Xe, or the adsorbed Xe would have been easier to desorb than degas. If this is the case then even the gas phase CO_2 would have easier access to that Xe than the dissolved Kr in the oil phase, resulting in high Xe concentrations in the gas phase in the early phase of injection. Based on this phenomenon it is also possible that a small amount of excess Kr is present in the system.

Re-dissolution of the degassed ASW-derived noble gases into the formation water in natural CO_2 reservoirs over geological time has been proposed as an explanation for elevated $^{20}Ne/^{36}Ar$ ratios (Gilfillan et al., 2008, 2009; Zhou et al., 2012). However, we can rule this out due to the large amount of injected CO_2 in a short period of time. Instead, the Kr and Xe noble gas data demonstrate that the injected CO_2 has contacted the different reservoir fluids to varying degrees throughout the Cranfield EOR reservoir over a range of timescales. It should be noted that the uncertainty of the composition of the in-situ gas (Table 4) may be significant if the O/W and G/W ratios are not constant throughout the field. However, with any O/W and G/W values prior to injection, the direction of the in-

situ gas and oil composition with respect to noble gases in Fig. 4 from ASW will not change. Consequently, uncertainty in the in-situ gas end-member will have little or no impact on the general trends observed and interpretations of these trends.

5.3. CO_2 dissolved from the gas phase

5.3.1. $CO_2/^3He$ vs. CO_2 concentration

The isotopic composition of He along with the observed CO_2 concentrations from the Cranfield EOR field demonstrate that five production well gas samples suffered significant CO_2 loss from the gas phase (Györe et al., 2015). Here, we show using more detailed modelling that CO_2 dissolution can be identified in nearly all of the produced gas samples.

Previous studies have shown that $CO_2/^3He$ of natural gases is a powerful tracer of the history of crustal natural gases that were derived from magmatic sources (Marty and Jambon, 1987; Marty et al., 1989; Sherwood Lollar et al., 1997; Trull et al., 1993). The $CO_2/^3He$ values from gas produced from the Cranfield field when compared to the CO_2 concentration, generally show mixing between Jackson Dome gas and pre-injection Cranfield gas (Fig. 5). A mixing line (continuous line) can be drawn between the Jackson Dome value ($CO_2 = 99\%$, $CO_2/^3He = 2.53 \times 10^9$, Zhou et al. (2012)) and the in-situ formation gas composition prior to injection of Jackson Dome CO_2 into the field ($CO_2/^3He = 1.9 \times 10^9$). The latter is calculated based on the CO_2 concentration (4%, Lu et al. (2012b)), the ^4He concentration (3×10^{-4} cm^3 STP/cm^3) and the $^3He/^4He$ ratio (0.05 R_A) of the in-situ natural gas prior to CO_2 injection (Györe et al., 2015). With the exception of 29-5 2012 all data are located on or below the mixing curve.

$CO_2/^3He$ values of the production well gases vary between 9.65×10^7 (28F-2 2009) and 4.01×10^9 (29-5 2012). This indicates that the majority of samples show CO_2 loss from the free supercritical phase. This is in agreement with the $^3He/^4He$ vs. CO_2 concentration in Fig. 5A in Györe et al. (2015), where almost all the samples show slightly lower CO_2 concentrations than predicted from the binary mixing relationship. The CO_2 loss in the five lowest

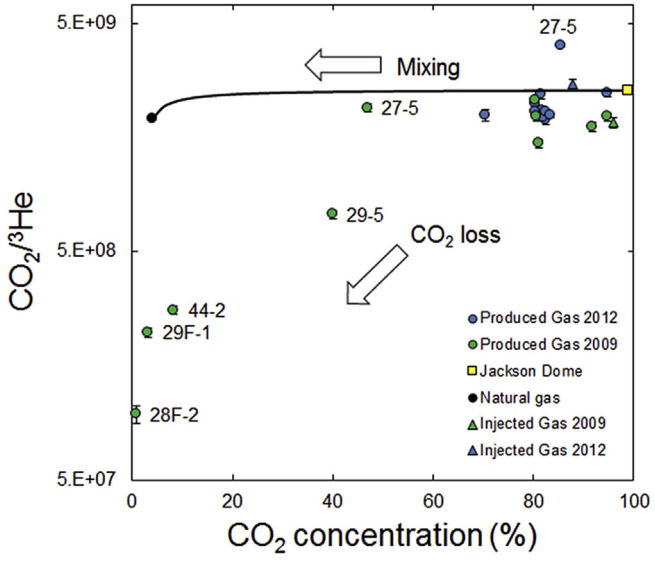

Fig. 5. Plot of $CO_2/^3He$ against CO_2 concentration for Cranfield well gases. A mixing curve is plotted between Jackson Dome (Zhou et al., 2012) and natural gas compositions. Data plotting below the mixing curve indicates CO_2 loss. The sample above the curve (27-5 2012) requires the addition of crustal CO_2, which may be derived from carbonate dissolution (see text). The five labelled wells in 2009 showed CO_2 loss in Györe et al. (2015). All data are after Györe et al. (2015). Uncertainties are 1σ.

CO_2 concentration samples was found to be between 28% (27-5 2009) and 93% (28F-2 2009) using the difference between measured $^3He/^4He$ and $^{40}Ar^*/^4He$ ratios from those predicted from the two mixing lines between the injected CO_2 and the prior-to-CO_2 injection end member (Györe et al., 2015). This has been calculated using the relative difference between the measured CO_2 concentration and the theoretical concentration at any given $^3He/^4He$ value according to the mixing curve. The CO_2 loss from the remaining samples can be calculated to be between 7% (29-5 2012) and 0.5% (45F-4 2012) (Table 5) using the same technique. The range of CO_2 loss is large, reflecting different degrees of CO_2 – water contact. The CO_2 loss in each well is in accordance with the non-radiogenic noble gas data above, which indicates that CO_2 has been in contact with the reservoir water and oil.

The $CO_2/^3He$ of well 29-5 2012 is 4.01×10^9 which is much higher than the Jackson Dome value of 2.53×10^9. This requires the addition of crustal CO_2, which has insignificant ^3He content. The addition of crustal derived CO_2, other than from mixing, can be explained by some carbonate dissolution and subsequent CO_2 degassing. The Cranfield reservoir contains an average of 1.1% calcite (Lu et al., 2012b). The dissolution of CO_2 will make the formation water a weak acid, thus more capable of dissolving calcite (Shevalier et al., 2013). Evidence of a small amount of carbonate dissolution has been identified by Lu et al. (2013) in the Cranfield field. To account for the high $CO_2/^3He$ ratio in sample 29-5 2012, 37% of the CO_2 would need to be derived from carbonate minerals although we are unable to rule out a degree of fractionation which could also increase the $CO_2/^3He$ value.

5.3.2. Stable isotope data

The fractionation of $\delta^{13}C_{CO2}$ and $CO_2/^3He$ has previously been used to distinguish between CO_2 precipitation to carbonate minerals and dissolution into formation water within natural CO_2 reservoirs (Dubacq et al., 2012; Gilfillan et al., 2009; Zhou et al., 2012). $CO_2/^3He$ has been recently examined at an active EOR site (Shelton et al., 2016); however, the $\delta^{13}C_{CO2}$ and $CO_2/^3He$ relationship has not yet been used in a field where CO_2 injection is active. Here, we investigate if the technique can be used to resolve the fate of the CO_2 injected into the Cranfield CO_2-EOR field. The $CO_2/^3He$ of a selection of wells from Cranfield is plotted against $\delta^{13}C_{CO2}$ in Fig. 6. The $CO_2/^3He$ composition of the CO_2 injected into Cranfield from Jackson Dome is 2.53×10^9 (Zhou et al., 2012) and −2.6‰, (Lu et al., 2012b), which was sampled from the bulk line bringing the CO_2 to the Cranfield site. Lu et al. (2012b) have reported the $\delta^{13}C$ of CO_2 from several production well gases that were sampled during the 2009 campaign for this study.

Using the $\delta^{13}C_{CO2}$ values from Lu et al. (2012b) and the ^3He concentrations from Györe et al. (2015) $CO_2/^3He$ and $\delta^{13}C$ of these CO_2 samples are also plotted in Fig. 6. The majority of the data plot below the bulkline composition, indicating a lowering of the $CO_2/^3He$ ratio without significant fractionation of the $\delta^{13}C_{CO2}$. The only exceptions to this trend is sample 28-2 2012, which is depleted in $^{13}C_{CO2}$ ($\delta^{13}C = -3.1$‰), relative to the majority of the samples, and 29F-1 2009 which exhibits both a depleted $\delta^{13}C_{CO2}$ (−4.81‰) and low $CO_2/^3He$ ratio (2.21×10^9) compared to the other samples. The dashed line in Fig. 6 is the modelled mixing between the injected Jackson Dome CO_2 and the Cranfield natural gas composition present prior to CO_2 injection (1.9×10^9 and -10.5‰, see above). No samples plot on this mixing line. The expected change of $CO_2/^3He$ and corresponding fractionation of $\delta^{13}C_{CO2}$ that would result from the dissolution of CO_2 into the formation water after Gilfillan et al. (2009) is shown as a continuous line in Fig. 6.

Dissolution of the free phase CO_2 into the formation water will form either H_2CO_3 or HCO_3^- depending on the pH. At the Cranfield reservoir temperature (120 °C, Lu et al. (2012b)) the fractionation

Table 5
The relative amount of lost CO_2 and theoretical CO_2 concentrations for Cranfield production wells. Lost CO_2 is expressed as a percentage, relative to the original CO_2 content. Original CO_2 content is also expressed as a percentage. Data have been re-calculated after Györe et al. (2015) (see Fig. 5 in Györe et al. (2015)): The previously plotted mixing curve has been modified in light of the new data presented here. NA: Not applicable.

Well	Latitude	Longitude	API number	Lost CO_2	Theoretical CO_2 content
28F-2 2009	31.57228	−91.15365	2,303,700,048	92.3	10.8
28F-2 2012				4.4	85.7
29F-1 2009	31.56536	−91.15032	2,303,700,046	83.7	20.2
29F-1 2012				2.2	72.1
29-5 2009	31.58094	−91.17919	2,300,100,173	28.2	55.7
29-5 2012				7.0	92.0
27-5 2009	31.58341	−91.15974	2,300,123,380	26.1	63.5
27-5 2012				NA	0.0
29-6 2009	31.57730	−91.17260	2,300,100,198	2.4	94.0
29-6 2012				NA	0.0
29-9 2009	31.57356	−91.16669	2,303,700,159	NA	0.0
29-9 2012				6.3	88.0
29-1 2009	31.58359	−91.17624	2,300,100,176	1.0	81.5
29-1 2012				4.3	85.7
27-3 2009	31.57988	−91.16013	2,300,103,394	6.6	86.7
27-3 2012				5.7	87.3
28-2 2009	31.57635	−91.15721	2,300,123,372	NA	0.0
28-2 2012				0.2	80.5
44-2 2009	31.57120	−91.18266	2,300,123,346	75.7	34.5
29-3 2009	31.58084	−91.16785	2,300,100,167	NA	0.0
24-3 2009	31.57933	−91.18393	2,300,100,172	NA	0.0
45F-4 2012	31.54144	−91.15343	2,303,700,336	0.5	82.0
32F-10 2012	31.55486	−91.15294	2,303,700,333	2.3	82.2
70-2 2012 (2/2)	31.53759	−91.15504	2,300,123,410	2.1	85.2

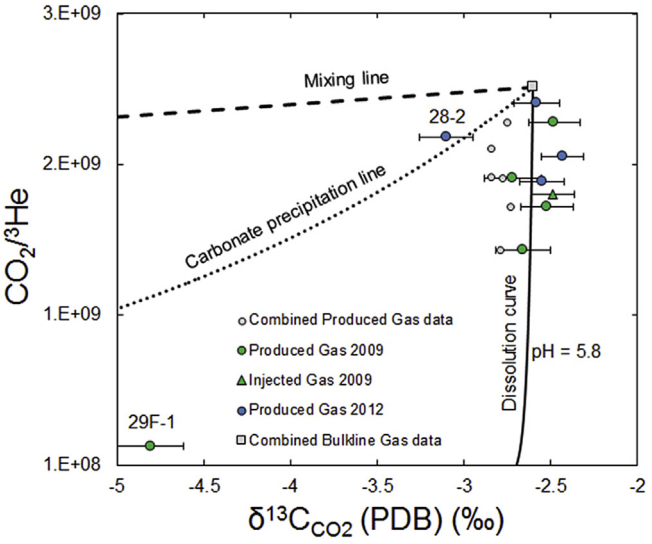

Fig. 6. $CO_2/^3He$ vs. $\delta^{13}C_{CO2}$ of Cranfield well gases. The majority of the data plot vertically below the bulkline composition on the dissolution curve (continuous line) at pH = 5.8 indicating that CO_2 has dissolved into water in those samples. Well 29F-1 could show dissolution (see text) but due to the low CO_2 concentration in that sample, both mixing with in-situ Cranfield gas and dissolution are apparent. Hence, there is uncertainty in the position of this sample (29F-1) on the dissolution curve and thus the pre-injection isotopic composition. Data from well 28-2 overlaps with the mineral precipitation line (dotted line) but a more likely explanation is that the presence of oil fractionates $\delta^{13}C_{CO2}$, which cannot be quantified. The sample located to the right of the dissolution curve could be explained by small variation of the local pH. Combined Produced Gas data are those wells where CO_2 concentrations and $\delta^{13}C_{CO2}$ are after Lu et al. (2012b) and He data are after Györe et al. (2015). Combined Bulkline Gas data's He data is from Zhou et al. (2012) and $\delta^{13}C_{CO2}$ is after Lu et al. (2012b). Uncertainties are depicted are 1σ.

factor between $CO_{2(g)}$ and H_2CO_3 is 0.7 (Myrttinen et al., 2014) and between HCO_3^- - $CO_{2(g)}$ is −0.2 (Mook et al., 1974). Henry's constants for He and CO_2 in water under the Cranfield reservoir conditions are calculated as 3745 and 178 atm kg/mol (Ballentine et al., 2002 and references therein). This allows the evolution of the $CO_2/^3He$ ratio as CO_2 dissolves to be constrained at any pH (Gilfillan et al., 2009). The dissolution curve has been calculated at pH = 5.8, which is the average reservoir pH in December 2009 (Lu et al., 2012b). Gases sampled in 2009, except for 29F-1, clearly show that the lost CO_2 has dissolved into the formation water confirming the previously outlined interpretation from the Kr-Ar-Ne data for the 2009 samples. The sample located right from the curve, outside the range of uncertainty could be explained by small variation of the local pH.

The simplest explanation for well 29F-1 plotting off the dissolution curve is the low CO_2 concentration. This means that there is evidence for both mixing with the pre-CO_2 injection reservoir gas and dissolution processes in the well 29F-1 dataset. While the mixing may be unimportant in the other samples, and therefore the dissolution can be modelled by having a well-defined starting point of the curve (Jackson Dome), the starting point of the dissolution curve for well 29F-1 gases can be anywhere along the mixing curve. The dissolution into the formation water may also explain why some data points on the $\delta^{13}C_{CO2}$–CO_2 diagram (Fig. 3 in Lu et al. (2012b)) are located to the lighter $\delta^{13}C_{CO2}$ side of the mixing curve. The dotted line shows the predicted trend for carbonate precipitation after Gilfillan et al. (2009). The fractionation factor between $CO_{2(g)}$ and $CaCO_3$ under reservoir conditions (see above) can be calculated to be 2.9 (Golyshev et al., 1981). The only sample which overlaps the precipitation trend line (dotted line) is from well 28-2 collected in 2012. The change in $CO_2/^3He$ and $\delta^{13}C_{CO2}$ in this sample could potentially be explained by precipitation of 12% of CO_2 as new carbonate mineral within the reservoir.

Despite extensive monitoring of the Cranfield reservoir fluid, geochemistry over the ~3 year period showed no evidence of carbonate precipitation (Lu et al., 2013). It is improbable that evidence of CO_2 precipitation should be recorded in only one sample if it was occurring across the reservoir. A more probable explanation is that greater relative CO_2 mixing with the oil present in the reservoir has occurred, which has fractionated the $\delta^{13}C_{CO2}$ as a result of greater contact of the CO_2 with the residual oil on the way to that well. Unfortunately, the isotopic fractionation of carbon isotope between $CO_{2(gas)}$ and dissolved CO_2 in crude oil has not yet been studied in

detail. However, on the bases of the $CO_{2(gas)}$ water system, it would be expected that partial CO_2 dissolution into the oil would preferentially extract ^{13}C from the CO_2 phase, resulting in a gas phase relatively depleted in ^{13}C. This fits the $\delta^{13}C_{CO2}$ fractionation trend observed to date. Due to the large amount of CO_2 injected in a relatively short period of time, we assume that the formation water is fully saturated and that the system is at or near to equilibrium. This assumption would make the system similar to natural gas reservoirs.

5.3.3. Estimation of the total amount of dissolved CO_2 over 18 months of injection

As previously outlined, the low $CO_2/^3He$ ratios indicate the loss of a proportion of the CO_2 through dissolution into the formation water, particularly in 2009. The isotopic composition of He after Györe et al. (2015) allow us to determine the relative proportion of CO_2 lost in each of the Cranfield production wells, and by comparing this to the amount of CO_2 produced from that well, the total amount of CO_2 lost to dissolution in 2009 is calculated. Summing the amount of CO_2 lost in the individual wells allows determination of the total amount of CO_2 lost to dissolution over the entire Cranfield CO_2-EOR field in 2009.

The total produced gas by December 2009 from each well on a monthly basis was provided by field operators during sampling for all wells. The numerical integral as the sum of the total produced gas by each well by the time of sampling is summarised in Table 6. The sum of the total produced gas can be calculated to be 8.14×10^7 m^3 STP.

In order to verify the total amount of produced gas, we now outline an independent means to estimate this value. The information regarding the volume of the injected gas (including Jackson Dome CO_2, mixed with recycled gas produced from the Cranfield EOR reservoir) via individual injection wells is available on a monthly basis from MSOGB (2015) (see online supplementary data). Using this data, the total volume of the injected gas up to the 1st of December 2009 via all the injection wells that were in production can be calculated to be 7.78×10^8 m^3 STP. The proportion of Jackson Dome CO_2 and recycled Cranfield gas injected into the reservoir is provided in Hovorka et al. (2013), allowing the total mass of CO_2 injected by the 1st of December 2009 to be calculated as 1.500 Mt, which is equivalent to 7.64×10^8 m^3 STP. This consisted of 1.337 Mt of Jackson Dome CO_2 and 0.163 Mt of CO_2 produced from the Cranfield reservoir, which was then re-injected.

The difference between the total injected gas, including both recycled CO_2 and CH_4 (7.78×10^8 m^3 STP from injection well data) and the injected CO_2 (7.64×10^8 m^3 STP) is 1.49×10^7 m^3 STP; this can be taken to be the total amount of produced and re-injected methane from the Cranfield reservoir. According to this mass balance calculation, the volumetric CO_2 concentration of the injected gas by December 2009 would be expected to be 98.1%, which is in a good agreement to that measured by Györe et al. (2015) from injection well 31F-1 collected in 2009 (96 ± 0.1%). The 0.163 Mt of recycled CO_2 is equivalent to 8.29×10^7 m^3 STP, which along with the produced CH_4 (1.49×10^7 m^3 STP) makes up the total amount of produced (and recycled) gas to be 9.78×10^7 m^3 STP, which is very close to the recorded value from the field of 8.14×10^7 m^3 STP.

If it is assumed that the CO_2 concentration is constant in a well during the 18 month observation period, the produced volume of the CO_2 in each well can be calculated using the CO_2 concentrations after Györe et al. (2015) and the volume of the produced gas provided by the field operator (Table 6). The sum of the calculated produced CO_2 is 5.35×10^7 m^3 STP, which would make the CO_2 concentration of the produced gas to be 65.7%. The CO_2 concentration of the produced gas can also be calculated from the mass balance (see above), where the total produced gas and the total produced methane were calculated to be 9.78×10^7 m^3 STP and 1.49×10^7 m^3 STP, and was estimated to be 84.7%. The difference may reflect the fact that production wells 29-11 and 29-13 were not in operation at the time of sampling in December 2009, which had produced significant amount of gas previously. If those two wells are excluded from the calculations (based on recorded produced gas data in Table 6), the total produced gas is 6.68×10^7 m^3 STP, which would make the CO_2 concentration of the produced gas 80% - only 4% different from the value calculated using the mass balance model.

Using the calculated CO_2 concentrations (see Table 5), the production, corrected for CO_2 loss can be calculated (see Table 6). The sum of the theoretical produced CO_2 is 5.51×10^7 m^3 STP, while the volume lost to dissolution can be calculated as 1.62×10^6 m^3 STP (theoretical produced CO_2− observed produced CO_2). Comparing this value to the total injected volume of CO_2 (7.78×10^8 m^3 STP) we can determine that ~0.2 ± 0.008% of the injected CO_2 has been lost to dissolution (assuming no uncertainty from i) the numerical models and ii) from the volumes and CO_2 concentrations of the produced gases in each well). It should be noted that the constant CO_2 concentration cannot be proved in the absence of time series data. However, by assuming the constant CO_2 concentration, we assume that the produced volumes of CO_2 presented here are maximums and therefore the percentage of dissolved CO_2 represents a minimum value. The degree of solubility trapping agrees with findings of Lu et al. (2013) who determined that there was limited evidence of substantial solubility trapped within the field.

Table 6
The production well data from the Cranfield EOR field at the time of the 2009 sampling campaign.

Production well	Total gas production (x 10^5)	CO_2 production (x 10^4)	Theoretical CO_2 production (x 10^4)
24–3	5.167	41.334	NA
29–1	25.215	203.488	205.505
29–6	69.036	633.754	648.942
29–9	108.546	1030.106	NA
29–3	26.596	212.768	NA
27–3	65.032	526.760	563.828
27–5	41.352	193.940	262.584
28–2	305.249	2454.206	NA
29–5	10.793	43.171	60.115
44–2	4.514	3.791	15.572
28F-2	0.888	0.080	0.959
29F-1	5.710	1.884	11.535
29–11	142.756	NA	NA
29–13	3.225	NA	NA

Gas productions are in m^3 STP and were recorded on the field during sampling.
NA: Not applicable.

The majority of the CO_2 is retained stratigraphically (or residually). This indicates that the same techniques could be used to quantify the fate of CO_2 injected into an engineered CO_2 storage site.

Unfortunately, we do not have access to the field production data set up to 2012, which prevents resolution of the amount of CO_2 lost to solubility trapping in 2012. However, we observe from the considerably smaller variation in $CO_2/^3He$ ratios relative to those of the injected CO_2 in the 2012 data set, that CO_2 dissolution is much less significant. This is to be expected as over the 2 years and 4 months since the 2009 samples were collected, some 3.5 million tonnes of additional CO_2 were injected into the field. It is clear from the small differences between the $CO_2/^3He$ ratios of a number of 2009 samples and that of the injected Jackson Dome CO_2, that the formation water was already highly saturated with respect to CO_2 in certain portions of the field, which would limit further CO_2 dissolution.

6. Conclusions

The non-radiogenic noble gases (^{20}Ne, ^{36}Ar, ^{84}Kr, ^{132}Xe) in well gases collected after 18 months of CO_2 injection from the Cranfield EOR field originate from the formation water, and have been extracted by different degrees of CO_2-formation water interaction, governed by the effectiveness of CO_2–water contact. This, combined with $CO_2/^3He$ and $\delta^{13}C_{CO2}$ measurements, provides evidence that the dissolution of CO_2 into formation water is responsible for the observed loss of free phase CO_2 relative to ^3He over the first 18 months of CO_2 injection. Combining the $CO_2/^3He$ ratios with $\delta^{13}C_{CO2}$ data allows constraint of the pH at which CO_2 dissolution is occurring which matches the previously measured average pH value from the field of 5.8 (Lu et al., 2012b).

Calculated production gas data, verified by a simple mass balance allows the He isotopic composition of well gases to be used to estimate the degree of solubility trapping throughout the reservoir. We find that ~0.2 ± 0.008% of the total stored retained CO_2 is dissolved into the formation water within the Cranfield reservoir. As previous geochemical modelling (e.g. Lu et al., 2013) and $\delta^{13}C_{CO2}$ measurements rule out observable mineral precipitation we conclude that the remainder of the injected CO_2 is retained by stratigraphic or residual trapping.

Well gas samples collected 45 months after the commencement of CO_2 injection show that the CO_2-oil interaction has become the main control on the noble gas composition of the gas produced. The lack of evidence of significant interaction between injected CO_2 and oil relative to the interaction between injected CO_2 and water during the earlier phase of oil recovery is not surprising as the Cranfield EOR field contains only residual oil which requires prolonged CO_2 interaction to liberate, with the formation water being much more accessible to the injected CO_2 at the start of the CO_2-EOR operation of the field. This study provides an excellent demonstration of how the naturally occurring noble gases could be employed to quantify the fate of CO_2 injected into an engineered CO_2 storage site.

Acknowledgements

This study was funded by EPSRC grant (EP/K036033/1) and University of Glasgow. Gilfillan was partially supported by an NERC Independent Research Fellowship (NE/G015163/1) and SCCS. We thank Denbury Resources Inc. for permission to undertake sampling at the Cranfield EOR field. We thank Susan Hovorka, Jiemin Lu and Jacob Anderson for providing detailed background information on the field and providing constructive comments, which significantly improved the manuscript. Two anonymous reviewers are thanked for their contribution which has significantly improved the manuscript. We are grateful to Luigia Di Nicola for invaluable help in the laboratories. We thank the Bureau of Economic Geology at the University of Texas at Austin and SECARB for giving access to the experiment.

Appendix A. Supplementary data

Supplementary data related to this article can be found at http://dx.doi.org/10.1016/j.apgeochem.2016.12.012.

Appendix 1. The concentration of ^{84}Kr in the DAS site relative to the Lower Tuscaloosa pool

The total mass of the added Kr into the DAS site was 7.3 kg (Lu et al., 2012a), which is equivalent to 1.95 m^3 STP (pV = nRT). The inherent Kr added with the Jackson Dome CO_2 via injection well 31F-1 into the DAS site can be calculated to be 0.001 m^3 STP, and therefore negligible in comparison to the amount of injected tracer. For the calculation, the volume of the injected gas after MSOGB (2015) and the concentration of ^{84}Kr of the Jackson Dome gas after Zhou et al. (2012) have been used. The 0.001 m^3 STP ^{84}Kr is obtained from the amount of injected gas via injector 31F-1 (MSOGB, 2015) and the concentration of ^{84}Kr of the Jackson Dome CO_2 (Zhou et al., 2012). In March 2012, the mass of the injected Jackson Dome CO_2 into the Lower Tuscaloosa pool is estimated to have been ~3.5 Mt (Hovorka et al., 2013) and the injected ^{84}Kr associated with this was 0.32 m^3 STP using the average measured concentration of ^{84}Kr in the Jackson Dome CO_2 of 1.782×10^{-10} cm^3 STP (Zhou et al., 2012). The area of the DAS site is 0.1 km^2 (Hosseini et al., 2013), while the Tuscaloosa pool's is 20.1 km^2 (see above). It is also assumed that the reservoir has equivalent depth and the rock has equivalent petrophysical properties in the main reservoir and in the DAS site. Thus, the concentration of ^{84}Kr in the DAS site relative to the main reservoir is 1219.

Appendix 2. Solubility controlled fractionation between three phases in a closed system.

The concentration of noble gas 'i' relative to Ar in each phase can be calculated by Eqs. (A.1-3) in a three-component system in equilibrium. o/O': oil, 'w/W': water, 'g/G': gas, 'K': Henry's constant, ASW: air saturated water. The ASW compositions, O/W, G/W and Henry's constants under reservoir conditions are in the text (after Bosch and Mazor, 1988).

$$\left(\frac{i}{Ar}\right)_g = \frac{\frac{K_i^w}{K_{Ar}^w}\left(\frac{i}{Ar}\right)_{ASW}}{1 + \frac{K_i^w}{K_{Ar}^w}\frac{K_{Ar}^o}{K_i^o}\frac{O}{W} + \frac{K_i^w}{K_{Ar}^w}\frac{G}{W}} \quad \text{Eq. (A.1)}$$

$$\left(\frac{i}{Ar}\right)_w = \frac{\left(\frac{i}{Ar}\right)_{ASW}}{1 + \frac{K_i^w}{K_{Ar}^w}\frac{K_{Ar}^o}{K_i^o}\frac{O}{W} + \frac{K_i^w}{K_{Ar}^w}\frac{G}{W}} \quad \text{Eq. (A.2)}$$

$$\left(\frac{i}{Ar}\right)_o = \frac{\frac{K_i^w}{K_{Ar}^w}\frac{K_{Ar}^o}{K_i^o}\left(\frac{i}{Ar}\right)_{ASW}}{1 + \frac{K_i^w}{K_{Ar}^w}\frac{K_{Ar}^o}{K_i^o}\frac{O}{W} + \frac{K_i^w}{K_{Ar}^w}\frac{G}{W}} \quad \text{Eq. (A.3)}$$

References

Aeschbach-Hertig, W., Peeters, F., Beyerle, U., Kipfer, R., 1999. Interpretation of dissolved atmospheric noble gases in natural waters. Water Resour. Res. 35,

2779–2792.
Alfi, M., Hosseini, S.A., 2016. Integration of reservoir simulation, history matching, and 4D seismic for CO_2-EOR and storage at Cranfield, Mississippi, USA. Fuel 175, 116–128.
Arts, R., Eiken, O., Chadwick, A., Zweigel, P., van der Meer, L., Zinszner, B., 2004. Monitoring of CO_2 injected at Sleipner using time-lapse seismic data. Energy 29, 1383–1392.
Assayag, N., Matter, J., Ader, M., Goldberg, D., Agrinier, P., 2009. Water–rock interactions during a CO_2 injection field-test: implications on host rock dissolution and alteration effects. Chem. Geol. 265, 227–235.
Ballentine, C.J., Burgess, R., Marty, B., 2002. Tracing fluid origin, transport and interaction in the crust. In: Porcelli, D., Ballentine, C.J., Wieler, R. (Eds.), Rev. Mineralogy Geochem. 47, 539–614. Noble Gases in Geochemistry and Cosmochemistry.
Ballentine, C.J., O'Nions, R.K., Coleman, M.L., 1996. A Magnus opus: helium, neon and argon isotopes in a North Sea oilfield. Geochim. Cosmochim. Acta 60, 831–849.
Ballentine, C.J., O'Nions, R.K., Oxburgh, E.R., Horvath, F., Deak, J., 1991. Rare gas constraints on hydrocarbon accumulation, crustal degassing and groundwater flow in the Pannonian Basin. Earth. Planet. Sci. Lett. 105, 229–246.
Ballentine, C.J., Schoell, M., Coleman, D., Cain, B.A., 2001. 300-Myr-old magmatic CO_2 in natural gas reservoirs of the west Texas Permian basin. Nature 409, 327–331.
Battani, A., Sarda, P., Prinzhofer, A., 2000. Basin scale natural gas source, migration and trapping traced by noble gases and major elements: the Pakistan Indus basin. Earth. Planet. Sci. Lett. 181, 229–249.
Berglund, M., Wieser, M.E., 2011. Isotopic compositions of the elements 2009 (IUPAC technical report). Pure Appl. Chem. 83.
Boreham, C., Underschultz, J., Stalker, L., Kirste, D., Freifeld, B., Jenkins, C., Ennis-King, J., 2011. Monitoring of CO_2 storage in a depleted natural gas reservoir: gas geochemistry from the CO2CRC Otway Project, Australia. Int. J. Greenh. Gas. Con 5, 1039–1054.
Bosch, A., Mazor, E., 1988. Natural gas association with water and oil as depicted by atmospheric noble gases: case studies from the southeastern Mediterranean Coastal Plain. Earth. Planet. Sci. Lett. 87, 338–346.
Choi, J.-W., Nicot, J.-P., Hosseini, S.A., Clift, S.J., Hovorka, S.D., 2013. CO2 recycling accounting and EOR operation scheduling to assist in storage capacity assessment at a U.S. gulf coast depleted reservoir. Int. J. Greenhouse Gas Control 18, 474–484.
Commer, M., Doetsch, J., Dafflon, B., Wu, Y., Daley, T.M., Hubbard, S.S., 2016. Time-lapse 3-D electrical resistance tomography inversion for crosswell monitoring of dissolved and supercritical CO_2 flow at two field sites: Escatawpa and Cranfield, Mississippi, USA. Int. J. Greenh. Gas. Con 49, 297–311.
Crovetto, R., Fernández-Prini, R., Japas, M.L., 1982. Solubilities of inert gases and methane in H_2O and in D_2O in the temperature range of 300 to 600 K. J. Chem. Phys. 76, 1077.
Dubacq, B., Bickle, M.J., Wigley, M., Kampman, N., Ballentine, C.J., Sherwood Lollar, B., 2012. Noble gas and carbon isotopic evidence for CO_2-driven silicate dissolution in a recent natural CO_2 field. Earth. Planet. Sci. Lett. 341–344, 10–19.
Emberley, S., Hutcheon, I., Shevalier, M., Durocher, K., Mayer, B., Gunter, W.D., Perkins, E.H., 2005. Monitoring of fluid–rock interaction and CO_2 storage through produced fluid sampling at the Weyburn CO_2-injection enhanced oil recovery site, Saskatchewan, Canada. Appl. Geochem 20, 1131–1157.
Freifeld, B.M., Trautz, R.C., Kharaka, Y.K., Phelps, T.J., Myer, L.R., Hovorka, S., Collins, D.J., 2005. The U-tube: a novel system for acquiring borehole fluid samples from a deep geologic CO_2 sequestration experiment. J. Geophys. Res. 110.
Giese, R., Henninges, J., Lüth, S., Morozova, D., Schmidt-Hattenberger, C., Würdemann, H., Zimmer, M., Cosma, C., Juhlin, C., 2009. Monitoring at the CO2 SINK site: a concept integrating geophysics, geochemistry and microbiology. Energy Procedia 1, 2251–2259.
Gilfillan, S.M.V., Ballentine, C.J., Holland, G., Blagburn, D., Sherwood Lollar, B., Scott, S., Schoell, M., Cassidy, M., 2008. The noble gas geochemistry of natural CO_2 gas reservoirs from the Colorado Plateau and Rocky Mountain provinces, USA. Geochim. Cosmochim. Acta 72, 1174–1198.
Gilfillan, S.M.V., Sherwood Lollar, B., Holland, G., Blagburn, D., Stevens, S., Schoell, M., Cassidy, M., Ding, Z., Zhou, Z., Lacrampe-Couloume, G., Ballentine, C.J., 2009. Solubility trapping in formation water as dominant CO_2 sink in natural gas fields. Nature 458, 614–618.
Gilfillan, S.M.V., Wilkinson, M., Haszeldine, R.S., Shipton, Z.K., Nelson, S.T., Poreda, R.J., 2011. He and Ne as tracers of natural CO_2 migration up a fault from a deep reservoir. Int. J. Greenh. Gas. Con 5, 1507–1516.
Golyshev, S.I., Padalko, N.L., Pechenkin, S.A., 1981. Fractionation of stable oxygen amd carbon isotope in carbonate systems. Geochem. Int.+ 18, 58–99.
Güleç, N., Hilton, D.R., 2016. Turkish geothermal fields as natural analogues of CO_2 storage sites: gas geochemistry and implications for CO_2 trapping mechanisms. Geothermics 64, 96–110.
Györe, D., Stuart, F.M., Gilfillan, S.M.V., Waldron, S., 2015. Tracing injected CO_2 in the Cranfield enhanced oil recovery field (MS, USA) using He, Ne and Ar isotopes. Int. J. Greenh. Gas. Con 42, 554–561.
Haszeldine, R.S., Quinn, Q., England, G., Wilkinson, M., Shipton, Z.K., Evans, J.P., Heath, J., Crossey, L., Ballentine, C.J., Graham, C.M., 2005. Natural geochemical analogues for carbon dioxide storage in deep geological porous reservoirs, a United Kingdom perspective. Oil Gas. Sci. Technol.- Rev. IFP 60, 33–49.
Hosseini, S.A., Lashgari, H., Choi, J.W., Nicot, J.-P., Lu, J., Hovorka, S.D., 2013. Static and dynamic reservoir modeling for geological CO2 sequestration at Cranfield, Mississippi, U.S.A. Int. J. Greenh. Gas. Con 18, 449–462.
Hovorka, S.D., Meckel, T.A., Treviño, R.H., 2013. Monitoring a large-volume injection at Cranfield, Mississippi—project design and recommendations. Int. J. Greenh. Gas. Con 18, 345–360.
Humez, P., Lions, J., Négrel, P., Lagneau, V., 2014. CO_2 intrusion in freshwater aquifers: review of geochemical tracers and monitoring tools, classical uses and innovative approaches. Appl. Geochem. 46, 95–108.
IPCC, 2005. IPCC special report on carbon dioxide capture and storage. In: Metz, B., Davidson, O., de Coninck, H.C., Loos, M., Meyer, L.A. (Eds.), Prepared by Working Group III of the Intergovernmental Panel on Climate Change. Cambridge University Press, Cambridge, United Kingdom/New York, NY, USA, p. 442.
Johnson, G., Dalkhaa, C., Shevalier, M., Nightingale, M., Mayer, B., Haszeldine, S., 2014. Pre-, syn- and post-CO_2 injection geochemical and isotopic monitoring at the pembina cardium CO_2 monitoring pilot, Alberta, Canada. Energy Procedia 63, 4150–4154.
Johnson, G., Mayer, B., Shevalier, M., Nightingale, M., Hutcheon, I., 2011. Tracing the movement of CO_2 injected into a mature oilfield using carbon isotope abundance ratios: the example of the Pembina Cardium CO_2 Monitoring project. Int. J. Greenh. Gas. Con 5, 933–941.
Kennedy, B.M., Reynolds, J.H., Smith, S.P., 1988. Noble gas geochemistry in thermal springs. Geochim. Cosmochim. Acta 52, 1919–1928.
Kennedy, B.M., Torgersen, T., van Soest, M.C., 2002. Multiple atmospheric noble gas components in hydrocarbon reservoirs: a study of the Northwest Shelf, Delaware Basin, SE New Mexico. Geochim. Cosmochim. Acta 66, 2807–2822.
Kharaka, Y.K., Specht, D.J., 1988. The solubility of noble gases in crude oil at 25-100°C. Appl. Geochem 3, 137–144.
Kipfer, R., Aeschbach-Hertig, W., Peeters, F., Stute, M., 2002. Noble gases in lakes and ground waters. In: Porcelli, D., Ballentine, C.J., Wieler, R. (Eds.), Reviews in Mineralogy & Geochemistry, vol. 47, pp. 615–700. Noble Gases in Geochemistry and Cosmochemistry.
Knauss, K.G., Johnson, J.W., Steefel, C.I., 2005. Evaluation of the impact of CO_2, co-contaminant gas, aqueous fluid and reservoir rock interactions on the geologic sequestration of CO_2. Chem. Geol. 217, 339–350.
Lu, J., Cook, P.J., Hosseini, S.A., Yang, C., Romanak, K.D., Zhang, T., Freifeld, B.M., Smyth, R.C., Zeng, H., Hovorka, S.D., 2012a. Complex fluid flow revealed by monitoring CO_2 injection in a fluvial formation. J. Geophys. Res. Solid Earth 117 (n/a-n/a).
Lu, J., Kharaka, Y.K., Thordsen, J.J., Horita, J., Karamalidis, A., Griffith, C., Hakala, J.A., Ambats, G., Cole, D.R., Phelps, T.J., Manning, M.A., Cook, P.J., Hovorka, S.D., 2012b. CO_2–rock–brine interactions in Lower Tuscaloosa Formation at Cranfield CO_2 sequestration site, Mississippi, U.S.A. Chem. Geol. 291, 269–277.
Lu, J., Kordi, M., Hovorka, S.D., Meckel, T.A., Christopher, C.A., 2013. Reservoir characterization and complications for trapping mechanisms at Cranfield CO_2 injection site. Int. J. Greenh. Gas. Con 18, 361–374.
Marty, B., Gunnlaugsson, E., Jambon, A., Oskarsson, N., Ozima, M., Pineau, F., Torssander, P., 1991. Gas geochemistry of geothermal fluids, the Hengill area, southwest rift zone of Iceland. Chem. Geol. 91, 207–225.
Marty, B., Jambon, A., 1987. $C/^3He$ in volatile fluxes from the solid Earth: implications for carbon geodynamics. Earth. Planet. Sci. Lett. 83, 16–26.
Marty, B., Jambon, A., Sano, Y., 1989. Helium isotopes and CO_2 in volcanic gases of Japan. Chem. Geol. 76, 25–40.
Mayer, B., Humez, P., Becker, V., Dalkhaa, C., Rock, L., Myrttinen, A., Barth, J.A.C., 2015. Assessing the usefulness of the isotopic composition of CO_2 for leakage monitoring at CO_2 storage sites: a review. Int. J. Greenh. Gas. Con 37, 46–60.
McCraw, C., Edlmann, K., Miocic, J., Gilfillan, S., Haszeldine, R.S., McDermott, C.I., 2016. Experimental investigation and hybrid numerical analytical hydraulic mechanical simulation of supercritical CO_2 flowing through a natural fracture in caprock. Int. J. Greenh. Gas. Con 48 (Part 1), 120–133.
Mook, W.G., Bommerson, J.C., Staverman, W.H., 1974. Carbon isotope fractionation between dissolved bicarbonate and gaseous carbon dioxide. Earth. Planet. Sci. Lett. 22, 169–176.
MSOGB, 2015. Mississippi Oil and Gas Board Online Database (Accessed in July, 2015). http://gis.ogb.state.ms.us/MSOGBOnline/.
Myrttinen, A., Becker, V., Mayer, B., Barth, J.A., 2014. Stable carbon isotope fractionation data between $H_2CO_3^*$ and $CO_{2(g)}$ extended to 120 °C. Rapid Commun. Mass Spectrom. 28, 1691–1696.
Myrttinen, A., Becker, V., van Geldern, R., Würdemann, H., Morozova, D., Zimmer, M., Taubald, H., Blum, P., Barth, J.A.C., 2010. Carbon and oxygen isotope indications for CO_2 behaviour after injection: first results from the Ketzin site (Germany). Int. J. Greenh. Gas. Con 4, 1000–1006.
Nimz, G.J., Hudson, G.B., 2005. The use of noble gas isotopes for monitoring leakage of geologically stored CO_2. In: Thomas, D.C., Benson, S.M. (Eds.), Carbon Dioxide Capture for Storage in Deep Geologic Formations. Elsevier, pp. 1113–1128.
Ozima, M., Podosek, F.A., 2001. Noble Gas Geochemistry, second ed. Cambridge University Press, Cambridge. 367.
Poreda, R.J., Farley, K.A., 1992. Rare gases in samoan xenolits. Earth. Planet. Sci. Lett. 113, 129–144.
Pujol, M., Marty, B., Burgess, R., 2011. Chondritic-like xenon trapped in Archean rocks: a possible signature of the ancient atmosphere. Earth Planet. Sci. Lett. 308 (3–4), 298–306.
Raistrick, M., Mayer, B., Shevalier, M., Perez, R.J., Hutcheon, I., Perkins, E., Gunter, B., 2006. Using chemical and isotopic data to quantify ionic trapping of injected carbon dioxide in oil field brines. Environ. Sci. Technol. 40, 6744–6749.
Romanak, K.D., Bennett, P.C., Yang, C., Hovorka, S.D., 2012. Process-based approach

to CO_2 leakage detection by vadose zone gas monitoring at geologic CO_2 storage sites. Geophys. Res. Lett. 39.
Serno, S., Johnson, G., LaForce, T.C., Ennis-King, J., Haese, R.R., Boreham, C.J., Paterson, L., Freifeld, B.M., Cook, P.J., Kirste, D., Haszeldine, R.S., Gilfillan, S.M.V., 2016. Using oxygen isotopes to quantitatively assess residual CO_2 saturation during the CO2CRC Otway Stage 2B Extension residual saturation test. Int. J. Greenh. Gas Control 52, 73–83.
Sathaye, K.J., Hesse, M.A., Cassidy, M., Stockli, D.F., 2014. Constraints on the magnitude and rate of CO_2 dissolution at Bravo Dome natural gas field. PNAS 111 (43), 15332–15337.
Scott, V., Gilfillan, S., Markusson, N., Chalmers, H., Haszeldine, R.S., 2013. Last chance for carbon capture and storage. Nat. Clim. Change 3, 105–111.
Shelton, J.L., McIntosh, J.C., Hunt, A.G., Beebe, T.L., Parker, A.D., Warwick, P.D., Drake, R.M., McCray, J.E., 2016. Determining CO_2 storage potential during miscible CO_2 enhanced oil recovery: noble gas and stable isotope tracers. Int. J. Greenh. Gas. Con 51, 239–253.
Sherwood Lollar, B., Ballentine, C.J., O'Nions, R.K., 1997. The fate of mantle-derived carbon in a continental sedimentary basin: integration of C/He relationships and stable isotope signatures. Geochim. Cosmochim. Acta 61, 2295–2307.
Sherwood Lollar, B., O'Nions, R.K., Ballentine, C.J., 1994. Helium and neon isotope systematics in carbon-dioxide-rich and hydrocarbon-rich gas reservoirs. Geochim. Cosmochim. Acta 58, 5279–5290.
Shevalier, M., Nightingale, M., Mayer, B., Hutcheon, I., Durocher, K., Perkins, E., 2013. Brine geochemistry changes induced by CO_2 injection observed over a 10 year period in the Weyburn oil field. Int. J. Greenh. Gas. Con 16, S160–S176.
Smith, S.P., Kennedy, B.M., 1983. The solubility of noble gases in water and in NaCl brine. Geochim. Cosmochim. Acta 47, 503–515.
Stalker, L., Boreham, C., Underschultz, J., Freifeld, B., Perkins, E., Schacht, U., Sharma, S., 2015. Application of tracers to measure, monitor and verify breakthrough of sequestered CO_2 at the CO2CRC Otway Project, Victoria, Australia. Chem. Geol. 399, 2–19.
Torgersen, T., Kennedy, B.M., 1999. Air-Xe enrichments in Elk Hills oil field gases: role of water in migration and storage. Earth. Planet. Sci. Lett. 167, 239–253.
Torgersen, T., Kennedy, B.M., van Soest, M.C., 2004. Diffusive separation of noble gases and noble gas abundance patterns in sedimentary rocks. Earth. Planet. Sci. Lett. 226, 477–489.
Trull, T., Nadeau, S., Pineau, F., Polvé, M., Javoy, M., 1993. C-He systematics in hotspot xenoliths: implications for mantle carbon contents and carbon recycling. Earth. Planet. Sci. Lett. 118, 43–64.
Warr, O., Rochelle, C.A., Masters, A., Ballentine, C.J., 2015. Determining noble gas partitioning within a CO_2–H_2O system at elevated temperatures and pressures. Geochim. Cosmochim. Acta 159, 112–125.
White, S.P., Allis, R.G., Moore, J., Chidsey, T., Morgan, C., Gwynn, W., Adams, M., 2005. Simulation of reactive transport of injected CO_2 on the Colorado Plateau, Utah, USA. Chem. Geol. 217, 387–405.
Wycherley, H., Fleet, A., Shaw, H., 1999. Some observations on the origins of large volumes of carbon dioxide accumulations in sedimentary basins. Mar. Petrol. Geol. 16, 489–494.
Zhou, Z., Ballentine, C.J., Kipfer, R., Schoell, M., Thibodeaux, S., 2005. Noble gas tracing of groundwater/coalbed methane interaction in the San Juan Basin, USA. Geochim. Cosmochim. Acta 69, 5413–5428.
Zhou, Z., Ballentine, C.J., Schoell, M., Stevens, S.H., 2012. Identifying and quantifying natural CO_2 sequestration processes over geological timescales: the Jackson Dome CO_2 Deposit, USA. Geochim. Cosmochim. Acta 86, 257–275.